Complete fusion of the 14N + 16O and 15N + 16O systems

C. Volant, S. Gary

Classification
Physics Abstracts
25.70

Complete fusion of the $^{14}N + {}^{16}O$ and $^{15}N + {}^{16}O$ systems

C. Volant and S. Gary

DPh-N/BE, CEN Saclay, BP 2, 91190 Gif-sur-Yvette, France

(*Reçu le 16 juin 1980, révisé le 25 septembre, accepté le 25 septembre 1980*)

Résumé. — Les sections efficaces des résidus d'évaporation issus de la fusion complète des systèmes $^{14}N + {}^{16}O$ et $^{15}N + {}^{16}O$ ont été mesurées à l'aide d'un télescope ΔE-E. Les distributions des différents éléments sont bien reproduites par des calculs d'évaporation basés sur la théorie statistique. Les fonctions d'excitation de fusion des deux systèmes sont très similaires contrairement à ce qui a été observé pour les systèmes $^{14}N + {}^{12}C$ et $^{15}N + {}^{12}C$. Les moments angulaires critiques de fusion déduits pour le système $^{14}N + {}^{16}O$ sont en accord avec ceux obtenus lors d'une analyse Hauser-Feshbach de la réaction $^{16}O(^{14}N, {}^{6}Li)^{24}Mg$. On compare aussi les données de ce travail avec celles obtenues pour le système $^{19}F + {}^{12}C$.

Abstract. — Cross sections for evaporation residues following the complete fusion of the $^{14}N + {}^{16}O$ and $^{15}N + {}^{16}O$ systems have been measured with a ΔE-E counter telescope. The distributions of the different elements are well reproduced by evaporation calculations based on the statistical theory. The fusion excitation functions for both systems have similar behaviours in contrast with what was observed for the $^{14}N + {}^{12}C$ and $^{15}N + {}^{12}C$ systems. Critical angular momenta for the fusion of the $^{14}N + {}^{16}O$ system agree with those obtained from a previous Hauser-Feshbach analysis of the $^{16}O(^{14}N, {}^{6}Li)^{24}Mg$ reaction. Comparisons with data for the $^{19}F + {}^{12}C$ system are also presented.

1. **Introduction.** — The studies of complete fusion between light ions have revealed a lot of unexpected features such as the large differences observed in the behaviours of the fusion excitation functions for close neighbouring systems [1, 2, 3]. One of the goals of the present work was to investigate further the influence of the valence nucleons on the fusion process, an influence which has first been put forward in the comparison of the $^{14}N + {}^{12}C$ and $^{15}N + {}^{12}C$ systems [2]. On the other hand, the direct measurements of the fusion cross sections for the $^{14}N + {}^{16}O$ system were also motivated by a possible comparison of the critical angular momenta for fusion with those deduced from an Hauser-Feshbach analysis of the cross sections of individual levels populated through the $^{16}O(^{14}N, {}^{6}Li)^{24}Mg$ reaction [4]. The values obtained by both methods agree for the $^{14}N + {}^{12}C$ system [5, 2] and it was interesting to pursue this comparison for another system. Furthermore, in reference [4], it was suggested that the fusion excitation function could present structures which have been observed so far only for systems where both partners are α-nuclei (^{12}C and ^{16}O). In the present experiments the atomic numbers of the detected evaporation residues have been identified individually and a comparison of the decays of the ^{30}P and ^{31}P compound nuclei with the results of a statistical evaporation model will also be made.

2. **Experimental procedure.** — The ^{14}N and ^{15}N beams from the FN tandem Van de Graaff of Saclay have been used with incident energies ranging from 30 to 64 MeV (^{14}N) and from 36 to 55 MeV (^{15}N). The targets were typically 100 $\mu g/cm^2$ thick and were made of silicon oxide with a thin gold layer of about 1 $\mu g/cm^2$ for monitoring purposes. The experimental set-up is described in reference [2] ; a solid state ΔE-E telescope ($\Delta E \sim 4\,\mu m$ thick) is used to detect the reaction products and a detector at fixed angle ($\theta_{lab} = 25°$) is used as a monitor.

A bidimensional spectrum is shown in figure 1. The elements of atomic numbers ranging from $Z = 8$ to 14 are well discriminated from each other. These nuclei were considered as evaporation residues resulting from the fusion of the nitrogen ions with the ^{16}O target and also with the carbon contaminant. It has been checked on a pure silicon target that the contribution of reactions on silicon to those events is negligible and that the fusion events on silicon are located well above the $^{14}N + {}^{16}O$ fusion events as shown

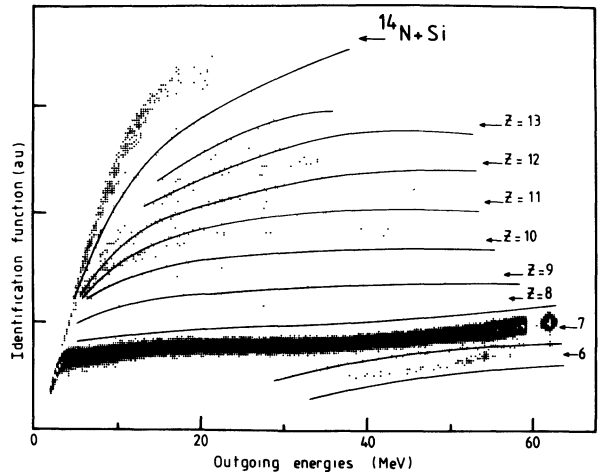

Fig. 1. — Typical ΔE-E matrix at E_{lab} = 64 MeV, θ_{lab} = 8° for the $^{14}N + ^{16}O$ system.

in the figure. A few carbon ions are also seen in figure 1, their energy spectra show some discrete peaks which are attributed to two-body reactions on oxygen because of their kinematical behaviour. They are disregarded in the present study.

Most of the events with $Z = 8$ and 9 in figure 1 are evaporation residues of the N + C fusion. The amount of the fusion cross section due to the carbon contribution was evaluated by measuring simultaneously the elastic scattering of the nitrogen ions on the carbon at energies where both elastic scattering and fusion cross sections have already been measured [2]. Two additional complete angular distributions of the fusion cross sections on a ^{12}C target have also been measured; the values integrated over angles ($^{14}N + ^{12}C$ at 30 MeV : $\sigma_{fus} = 770 \pm 54$ mb and $^{15}N + ^{12}C$ at 55 MeV : $\sigma_{fus} = 1\,091 \pm 76$ mb) are in good agreement with the excitation functions of reference [2].

3. **Experimental results.** — 3.1 ANGULAR DISTRIBUTIONS. — Angular distributions of elements with $Z \geqslant 7$ were measured from $\theta_{lab} = 3.5°$ to 25° for the $^{14}N + ^{16}O$ reaction at bombarding energies of 30, 37, 47 and 58.25 MeV. Furthermore the excitation function of the fusion yield at $\theta_{lab} = 8°$ was obtained from 30 to 64 MeV in steps of approximately 1 MeV.

For the $^{15}N + ^{16}O$ reaction similar angular distributions have been obtained at 36, 47 and 55 MeV, the excitation function at $\theta_{lab} = 8°$ has been measured from 36 to 55 MeV by steps of 2 MeV.

Figure 2 shows the angular distributions for the sum of the evaporation residues and figure 3 for each of the Z-residues; in the $^{14}N + ^{16}O$ case at 30 MeV the various Z were not resolved. These angular distributions exhibit patterns commonly observed in this kind of measurements : the $d\sigma/d\theta$ maxima for the elements involving α-emission in the decay chain are shifted to larger angles than for those involving only nucleons, and the angular distributions are broadened for elements far from the compound nucleus.

The absolute scale for cross sections is determined from optical model fits of the N + O elastic scattering data obtained simultaneously with the fusion data.

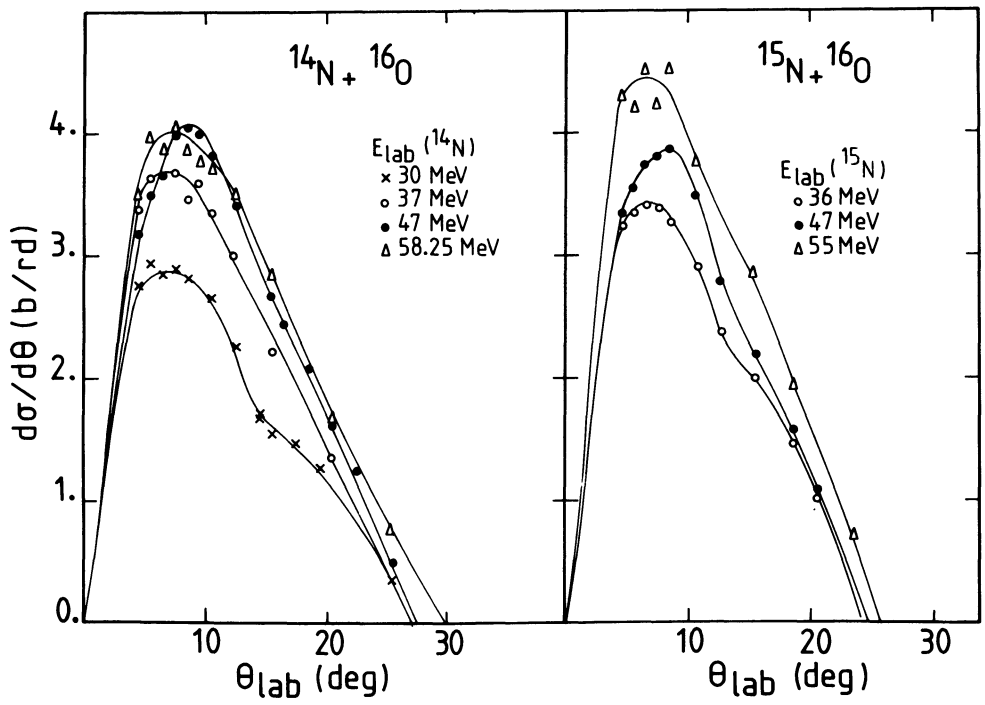

Fig. 2. — Angular distributions of the total fusion for the $^{14}N + ^{16}O$ and $^{15}N + ^{16}O$ systems at different energies. The curves are drawn to guide the eye.

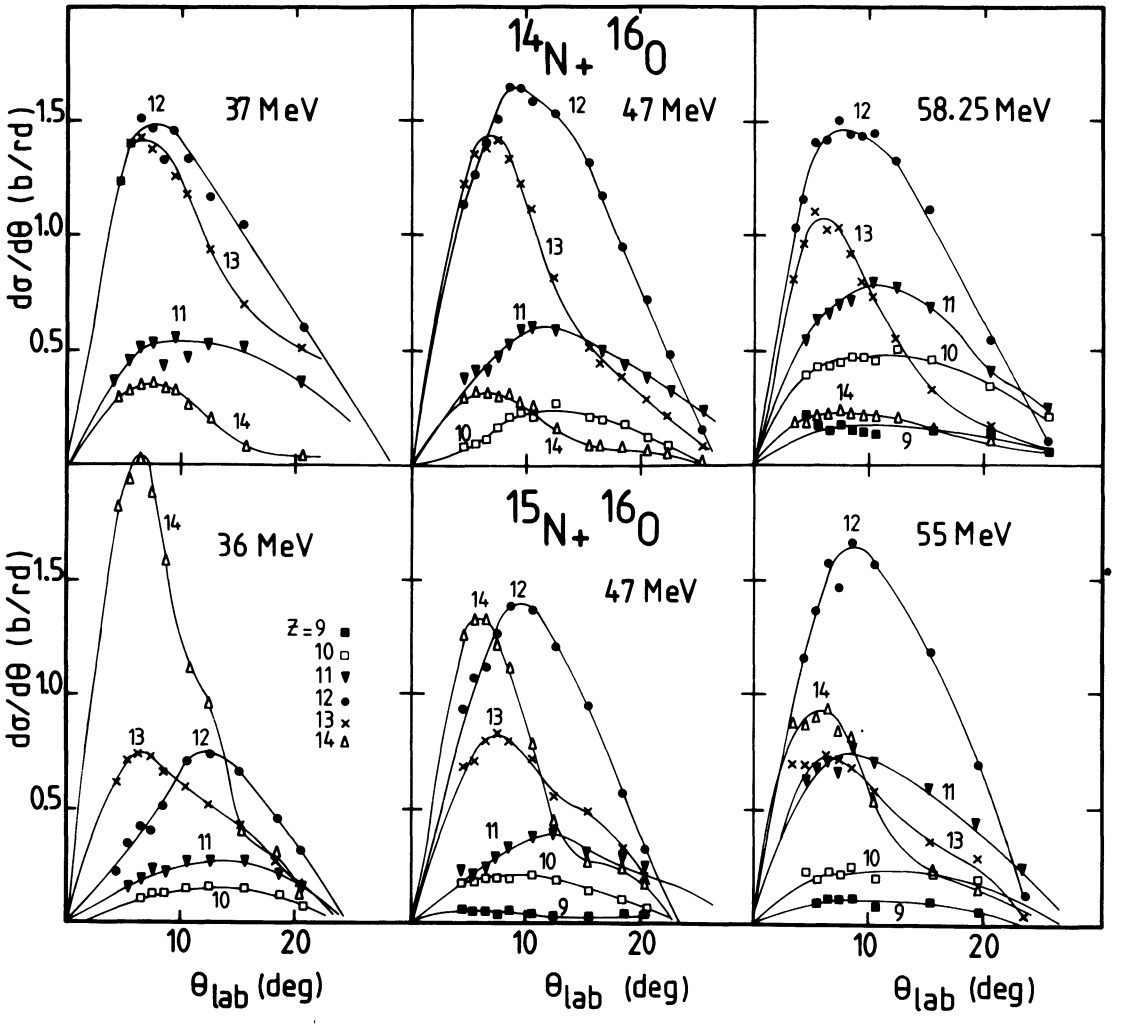

Fig. 3. — Angular distributions of the evaporation residues for the ^{14}N + ^{16}O and ^{15}N + ^{16}O systems at different energies. The curves are drawn to guide the eye.

This scaling depends on the optical model parameters since at the very forward angles the ^{16}O peak cannot be separated from the Si peak and thus the normalization cannot be based on the forward Rutherford elastic scattering. We found that the energy dependent Siemssen's parameters [6] fit very well our angular distributions at each incident energy and we estimate the uncertainties of this procedure at 5-6 %. We also took into account three other types of errors : the uncertainty on the relative thickness of the carbon contaminant, the errors on the N + C measurements [2] and, finally, the error on the integration of the cross sections due to the extrapolation of the fusion angular distributions at small and very large angles. These uncertainties lead us to estimate that the absolute values of the total fusion cross sections are determined within about 10 %. The results are given in table I together with the integrated cross sections for the various elements. Due to additional errors in the statistics and some separation problems, the cross sections have uncertainties of about 15-20 % for Z = 12, 13, 14 except for the small cross sections

Table I. — *Cross sections of the different elements and of the total fusion* σ_{fus} *(errors are discussed in the text).* σ_R *are the reaction cross sections calculated from an optical model using the parameters of reference* [6]. *Cross sections are in* mb *and energies in* MeV.

	$^{14}N + ^{16}O$ (a) → $^{30}P^*$			$^{15}N + ^{16}O$ → $^{31}P^*$		
E_{lab}	37	47	58.25	36	47	55
E_{cm}	19.73	25.07	31.07	18.58	24.26	28.39
E_x	38.06	43.40	49.40	38.39	44.06	48.19
σ_R	1 075	1 273	1 405	1 055	1 286	1 394
σ_{fus}	950	1 100	1 145	850	960	1 130
Z=14	61	68	26	362	242	181
13	340	308	222	170	193	162
12	373	455	411	181	329	405
11	175	194	248	83	123	216
10		60	177	45	57	83
9		15	59	13	13	42
8						40

(a) At E_{lab} = 30 MeV only the total cross section σ_{fus} integrated over Z has been measured (σ_{fus} = 772 ± 80 mb).

of the $Z = 14$ in the $^{14}N + ^{16}O$ case ($\sim$ 30-40 %). Errors are also large (20-40 %) for the elements of $Z \leqslant 11$ for which important relative contributions of the ^{12}C contaminant are subtracted.

3.2 EXCITATION FUNCTIONS. — The excitation functions of the integrated fusion yields were measured at $\theta_{lab} = 8°$. We obtained the relative cross sections by reference to the elastic Au yield in the monitor which was assumed to follow the Rutherford scattering. The stability of the target composition has been checked by repeating a few times measurements at the same energy throughout the excitation function; corrections for carbon build-up have also been made. The results are then normalized to the cross sections determined from complete angular distributions. At the last step of the data analysis, the integrated cross sections were obtained by assuming that the ratio of the yield at one angle to the integrated fusion yield changes linearly as a function of energy. The errors on the relative magnitude of the cross sections for a given system are approximately 5 % and the *ratio* of the cross sections of the ^{14}N and ^{15}N induced reactions is determined within an accuracy of 7 %.

We present the result of the total fusion cross sections in figure 4 while figure 5 shows the excitation function for the most populated elements in the two studied systems.

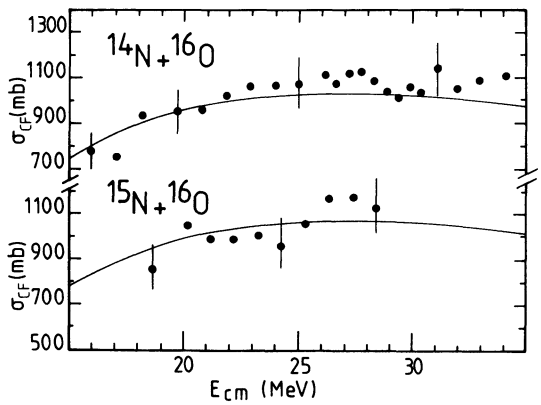

Fig. 4. — Total fusion cross sections as a function of cm energy. The curves are the results of a calculation using the model of reference [18]. Error bars are drawn only for the points where angular distributions have been measured.

4. Discussion of the results. — 4.1 DECAY OF THE COMPOUND NUCLEI. — The excitation functions drawn in figure 5 for each Z-residue show that the two compound nuclei behave quite differently. In the $^{14}N + ^{16}O$ case (^{30}P compound nucleus) the decay pattern is dominated at all energies by channels involving α-emission, whereas the ^{31}P compound nucleus decay shows a changing pattern : at low energy the nucleon emission dominates and the α-emission is growing up with energy and becomes predominant at high energy.

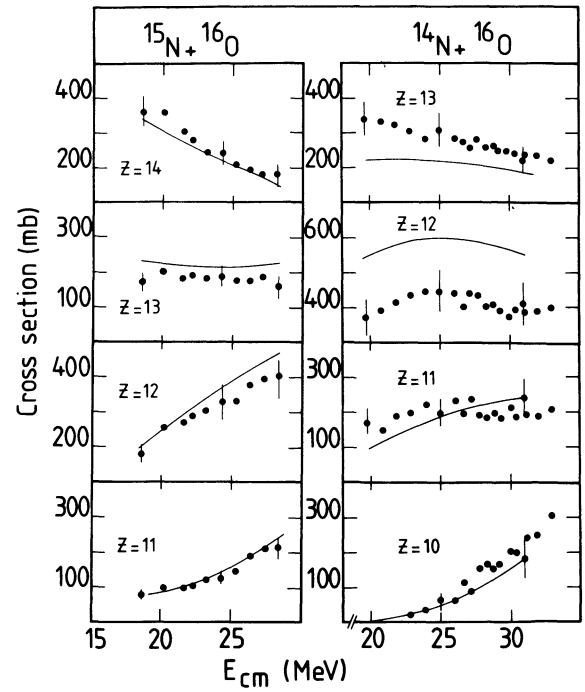

Fig. 5. — Excitation functions of the most populated evaporation residues for the $^{14}N + ^{16}O$ and $^{15}N + ^{16}O$ systems. The curves are the results of calculations using the evaporation code CASCADE [7].

These trends are very well reproduced by statistical decay computations performed using the CASCADE code [7] (full curves in figure 5). The agreement with the relative populations of the various elements is very nice for the $^{15}N + ^{16}O$ system. But although the trend is also well given for the $^{14}N + ^{16}O$ system, the $Z = 12$ is overestimated and the $Z = 13$ is underestimated, the less populated elements ($Z = 14$ and 9), not drawn in the figure, account by about 100 mb at higher energies and are also underpredicted. The parameters in the calculations are those used by Pühlhofer for the $^{19}F + ^{12}C$ system [7] (same compound nucleus as $^{15}N + ^{16}O$) and it has been shown that they give good agreement with a large amount of data [8]. In these calculations, the only variable is the maximum angular momentum of the compound nucleus which is determined according to the experimental fusion cross section. Because we feel that the set of parameters has to be considered as a whole, no attempt has been made to modify some characteristics in the decay chain in order to improve the agreement in the ^{30}P case.

Although some details are not totally reproduced it can be concluded that the statistical calculations are in good agreement with these data and that fully equilibrated compound nuclei have been formed. In the $^{19}F + ^{12}C$ system a few discrepancies with the calculations at high bombarding energies [9] have been interpreted as evidence for incomplete fusion, however the energy range studied in the present work is lower and such processes are expected to be negligible.

4.2 TRENDS OF THE TOTAL FUSION CROSS SECTIONS WITH BOMBARDING ENERGY. — The excitation functions reported in figure 4 show that the two systems behave quite similarly. The absolute cross sections are nearly the same in the energy range we studied and this is in contrast with the $^{14}N + ^{12}C$ and $^{15}N + ^{12}C$ data [2] which differ by more than 10%. It is likely that some properties specific to the ^{12}C nucleus have to be taken into account in order to explain the differences observed in the $N + ^{12}C$ systems.

A few accidents in the smooth behaviour of the excitation functions in figure 4 seem to exist, however their magnitude does not exceed the present experimental uncertainties and we are not able to conclude if there is some similarity with the neighbouring system $^{16}O + ^{16}O$ [3, 10].

One can mention that the maximum cross sections measured for the $^{14}N + ^{16}O$ and $^{15}N + ^{16}O$ systems exceed 1 100 mb; this observation, together with other measurements [11, 12], is in contradiction with the suggested influence of shell effects on σ_{fus}^{max} [13].

The fusion data for the $^{14}N + ^{16}O$ system are also plotted *versus* $1/E_{cm}$ (E_{cm} is the centre of mass energy) in figure 6, where low energy data from reference [14] are also reported. The dashed curve is calculated using the model of Glas and Mosel with the following parameters in the notations of reference [15] : $V_B = 8.8$ MeV, $r_B = 1.5$ fm, $\hbar\omega = 2$ MeV, $V_{cr} = 0$ MeV (assumed) and $r_{cr} = 1.18$ fm. The parameters V_B and r_B, which govern the low energy part, are those used in reference [14]; their values agree with the systematic made by Kovar *et al.* [3]. At high energy not enough data are available to allow an independent determination of V_{cr} and r_{cr}.

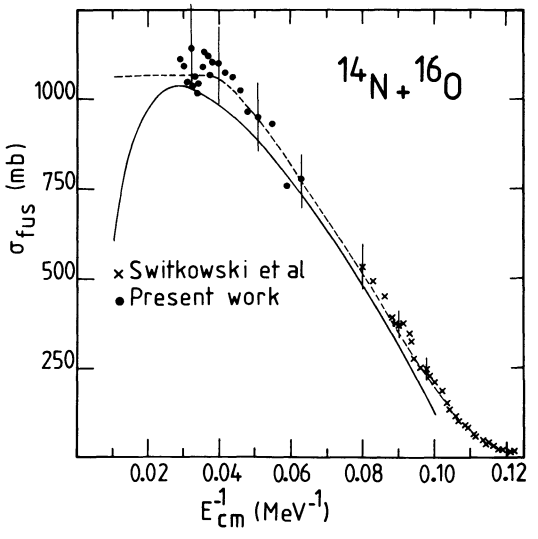

Fig. 6. — Fusion cross sections *versus* $1/E_{cm}$ (E_{cm} is the energy in the centre of mass) for the $^{14}N + ^{16}O$ system. Low energy data (crosses) are from reference [14], points are from the present work. The dashed curve is calculated from reference [15] with the parameters given in the text; the full curve is taken from the work of Birkelund *et al.* [16].

Several macroscopic models can be found in the literature, which permit the calculation of the energy dependence of the fusion cross sections [16]. They account reasonably well for the bulk of existing data although, very often they fail to reproduce accurately individual systems. An example of such predictions is given by the full curve of figure 6, which is taken from the recent work of Birkelund *et al.* [16]. The fusion cross sections are calculated using the proximity potential with a one-body friction and the agreement with the data is fair, although some increase of the nuclear radius could improve the fit.

Attempts to introduce some properties relevant to the nuclear structure have recently been made by Horn and Ferguson [17] which parametrized the fusion cross sections in two terms : one characterizing the compound nucleus and one the entrance channel. A modification of this model has been proposed by Lozano and Madurga [18] which use nuclear densities rather than charge densities; the results of such calculations are the solid curves drawn in figure 4 which fit quite well the experimental data.

4.3 CRITICAL ANGULAR MOMENTA. — Using the sharp cut-off approximation and assuming that all the low partial waves lead to fusion, the fusion cross section σ_{fus} can be written as :

$$\sigma_{fus}(E_{cm}) = \pi\lambda\!\!\!^{-2}(l_{cr} + 1)^2 \qquad (1)$$

where $\lambda\!\!\!^{-}$ is the reduced wavelength and l_{cr} the critical angular momentum. Hence, for each incident energy E_{cm}, one can obtain the maximum angular momentum l_{cr} reached for the corresponding excitation energy of the compound nucleus $E_x = E_{cm} + Q$ (Q is the usual Q-value for the compound nucleus formation). A plot of E_x *versus* $l_{cr}(l_{cr} + 1)$ is shown in figure 7*a* for the $^{14}N + ^{16}O$ data; on this figure are also shown (white rectangles) the critical angular momenta deduced from the Hauser-Feshbach analysis of the $^{16}O(^{14}N, ^{6}Li)^{24}Mg$ reaction leading to discrete ^{24}Mg levels [4]. The present data are in good agreement with the earlier analysis as it was the case for the $^{14}N + ^{12}C$ system [5, 2]; however the tendency for a structure suggested in [4] is not observed here at least within our experimental uncertainties.

Formally one can write [9] :

$$E_x = Q + V + \frac{\hbar^2}{2\mathfrak{I}} l_{cr}(l_{cr} + 1). \qquad (2)$$

This equation can describe two types of behaviour :

— The fusion is limited by the entrance channel and hence the moment of inertia might be expressed as $\mathfrak{I} = \mu R_B^2$ or μR_{cr}^2 (μ is the reduced mass) and V is the interaction potential (V_B or V_{cr}) between the two nuclei.

— The fusion is limited by the compound nucleus properties and $\mathfrak{I}$ and V can be interpreted respectively

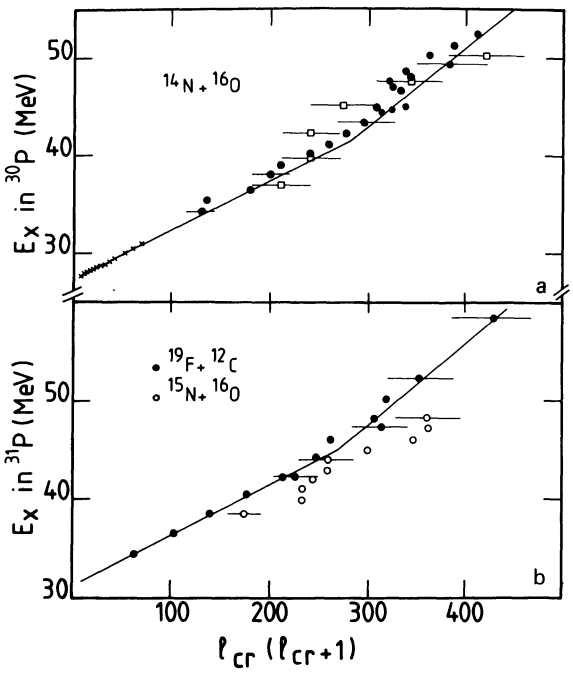

Fig. 7. — Critical angular momenta for fusion as a function of the compound nucleus excitation energy. *a*) $^{14}N + ^{16}O$ system, black points are from the present work, the white rectangles are from reference [4]. Straight lines are drawn from equation (2) with $2\,\mathfrak{I}_B/\hbar^2 = 19.6$ MeV^{-1} (low energy) and $2\,\mathfrak{I}_{cr}/\hbar^2 = 12.12$ MeV^{-1} (high energy). *b*) ^{31}P compound nucleus populated through the $^{19}F + ^{12}C$ [9] and $^{15}N + ^{16}O$ entrance channels. Full lines are from reference [9].

as the moment of inertia and the deformation energy of the compound nucleus.

We can indeed draw two straight lines through the points of figure 7*a*. The parameters V are those used in the analysis by the model of Glas and Mosel (Fig. 6) and the $\mathfrak{I}$'s are deduced from the radii parameters ; this can be done by using equations (1) and (2) in the limit of $l_{cr} \gg 1$ and the asymptotical behaviours of σ with energy given in reference [15]. In the low excitation energy region, the fusion is limited by the entrance channel properties. However, in the high energy part as usual for these light systems, it is not clear where does the limitation come from : it can be either an influence of the incoming channel, parametrized for example by a critical distance [19] or some characteristics of the compound nucleus. $\mathfrak{I}$ could then be interpreted as a moment of inertia of the ^{30}P compound nucleus ; the value $2\,\mathfrak{I}_{cr}/\hbar^2 = 12.12$ MeV^{-1} is very similar to the one deduced for the ^{31}P compound nucleus from the study of the $^{19}F + ^{12}C$ system [9].

The same plot for the $^{15}N + ^{16}O$ system is given in figure 7*b* and a comparison is done with the data on the $^{19}F + ^{12}C$ system for which the two thick straight lines given by the equation (2) are taken from reference [9]. In the low energy region, entrance channel effects like the number of available partial waves in the incoming channel could explain that the $^{15}N + ^{16}O$ points lie lower than the $^{19}F + ^{12}C$ points ; unfortunately data on the $^{15}N + ^{16}O$ system are still missing in the high energy part and one cannot conclude if, in this region, the fusion is governed by the entrance channel properties or if the same limit is obtained in the compound nucleus through different entrance channels as discussed recently [20, 12].

Acknowledgments. — We wish to thank M. Conjeaud, F. Saint-Laurent and J. P. Wieleczko for their helps during the experiments and their suggestions. We also gratefully acknowledge the help of S. Janouin during the data analysis.

References

[1] Sperr, P., Braid, T. H., Eisen, H., Kovar, D. G., Prosser, F. W., Schiffer, J. P., Tabor, S. L. and Vidgor, S., *Phys. Rev. Lett.* **37** (1976) 321.

[2] Conjeaud, M., Gary, S., Harar, S. and Wieleczko, J. P., *Nucl. Phys.* **A 309** (1978) 515.

[3] Kovar, D. G., Geesaman, D. F., Braid, T. H., Eisen, H., Henning, H., Ophel, T. R., Paul, M., Rehm, K. E., Sanders, S. J., Sperr, P., Schiffer, J. P., Tabor, S. L., Vigdor, S. and Zeidman, B., *Phys. Rev.* **C 20** (1979) 1305.

[4] Volant, C., Conjeaud, M., Harar, S. and Da Silveira, E. F., *J. Physique* **38** (1977) 1179.

[5] Volant, C., Conjeaud, M., Harar, S., Lee, S. M., Lépine, A. and Da Silveira, E. F., *Nucl. Phys.* **A 238** (1975) 120.

[6] Siemssen, R. H., *Heavy ion scattering*, Argonne 25-26 march 1971, ANL 7837 (1971) 145.

[7] Pühlhofer, F., *Nucl. Phys.* **A 280** (1977) 267 and private communication.

[8] Volant, C. and Wieleczko, J. P., *Proceedings of the XVII International Winter Meeting on Nuclear Physics*, Bormio, January 1979 (Edited by I. Iori, Milan), p. 308.

[9] Kohlmeyer, B., Pfeffer, W. and Pühlhofer, F., *Nucl. Phys.* **A 292** (1977) 288.

[10] Fernandez, B., Gaarde, C., Larsen, J. S., Pontoppidan, S. and Videbaek, F., *Nucl. Phys.* **A 306** (1978) 259.

[11] Gomez del Campo, J., Dayras, R. A., Biggerstaff, J. A., Shapira, D., Snell, A. H., Stelson, P. H. and Stokstad, R. G., *Phys. Rev. Lett.* **43** (1979) 26.

[12] Wieleczko, J. P., Harar, S., Conjeaud, M. and Saint-Laurent, F., *Phys. Lett.* **93B** (1980) 35.

[13] Schiffer, J. P., *Proceedings of the International Conference on Nuclear Structure*, Tokyo, September 1977, p. 9.

[14] Switkowski, Z. E., Stokstad, R. G. and Wieland, R. M., *Nucl. Phys.* **A 279** (1977) 502.

[15] Glas, D. and Mosel, U., *Nucl. Phys.* **A 237** (1975) 429.

[16] Wilczynski, J., *Nucl. Phys.* **A 216** (1973) 386.
Bass, R., *Phys. Rev. Lett.* **39** (1977) 265.
Krappe, H. J., Nix, J. R. and Sierk, A. J., *Phys. Rev.* **C 20** (1979) 992.
Vaz, L. C. and Alexander, J. M., *Phys. Rev.* **C 18** (1978) 2152.
Birkelund, J. R., Tubbs, L. E., Huizenga, J. R., De, J. N. and Sperber, D., *Phys. Rep.* **C 56** (1979) 107.

[17] Horn, D. and Ferguson, A. J., *Phys. Rev. Lett.* **41** (1978) 1529.

[18] Lozano, M. and Madurga, G., *Phys. Lett.* **90B** (1980) 50.

[19] Galin, J., Guerreau, D., Lefort, M. and Tarrago, X., *Phys. Rev.* **C 9** (1974) 1018.

[20] Saint-Laurent, F., Conjeaud, M., Harar, S., Loiseaux, J. M., Menet, J. and Viano, J. B., *Nucl. Phys.* **A 237** (1979) 517.